Progress In Electromagnetics Research, PIER 85, 39–67, 2008

EM SCATTERING FROM A LONG DIELECTRIC CIRCULAR CYLINDER

W. Z. Yan, Y. Du, H. Wu, and D. W. Liu

The Electromagnetics Academy at Zhejiang University
Zhejiang University
Hangzhou, Zhejiang 310058, China

B. I. Wu

Department of Electrical Engineering and Computer Science
Massachusetts Institute of Technology
Cambridge, MA 02139, USA

Abstract—A new iterative technique based on the T-matrix approach is proposed for the electromagnetic scattering by dielectric cylinders, in particular cylinders with large aspect ratios. For such cases the conventional T-matrix approach fails. We use hypothetic surfaces to divide a cylinder into a cluster of N identical sub-cylinder, for each the T matrix can be directly calculated. Since any two neighboring sub-cylinder are touching via the division interface, the conventional multi-scatterer equation method is not directly applicable. The coupling among sub-cylinder and boundary conditions at the interfaces are taken care of in our approach. The validity of the proposed method is demonstrated through agreement between theoretical predictions and numerical simulations as well as measurements for scattering from dielectric circular cylinders with finite length. The results clearly demonstrate that the new iterative technique can extend regular T-matrix approach to solve cylindrical cases with large aspect ratio.

1. INTRODUCTION

There has been growing interest in the investigation of vegetation using polarimetric remote sensing techniques. During the past several decades, a number of theoretical models have been constructed to study the scattering mechanisms in the vegetation medium and are very useful for forest stand or short crops [1–5]. Usually, these

approaches treat the vegetation medium as a random collection of discrete scatterers with different sizes, shapes and orientations. For instance, the branches and trunks are usually modelled as finite dielectric cylinders, and in coniferous vegetation needles are used to model leaves. Determining the electromagnetic properties of those key constituents such as branches and trunks requires knowledge of the scattering properties of dielectric cylinders [6–19]. In addition, in studying scattering and absorption of electromagnetic waves from ice needles in clouds, the dielectric cylinder are also used to model those needles [20]. Thus, finding an effective method to calculate the electromagnetic scattering by dielectric finite cylinders motivated many authors. Because an exact analytical solution for the scattering from finite cylinders does not exist, several approximations have been proposed [21–24]. Among them is the generalized Rayleigh-Gans (GRG) approximation, which was widely applied in the studies of the vegetation samples [22, 23]. It approximates the induced current in a finite cylinder by assuming infinite length. Therefore, this method is valid for a needle shaped scatterer with radius much smaller than the wavelength. Whereafter, Stiles and Sarabandi [24] proposed a more general solution for long and thin dielectric cylinders of arbitrary cross section, but still limited to small cross sections. Nevertheless, it should be noted that the solutions of such approximate methods in general fail to satisfy the reciprocity theorem.

In a more general setting, a semi-analytical method named T-matrix approach, originally introduced by Waterman [25] and is based on the extended boundary condition method (EBCM), is one of the most powerful and widely used tools for rigorously computing volume electromagnetic scattering based on Maxwell's equations and has been applied to particles of various shapes, such as spheroids, finite cylinders, Chebyshev particles, cubes, clusters of spheres, and so on [26–31]. In applying extended boundary condition to calculate the T matrix that relates the exciting field and scattered field, the exciting field is assumed to be inside the inscribing sphere and the scattered field outside the circumscribing sphere, respectively. However, for particles with extreme geometries represented by very large aspect ratios, regular EBCM is reported to suffer from convergence problems [32]. Physically, this ill-conditioning procedure stems from the fact that, since the exciting field is assumed to be inside the inscribing sphere, for cases of extreme geometries, the exciting fields will not be accurate representative of surface currents. Nor will the scattered fields.

One approach for overcoming the problem of numerical instability in computing the T matrix for spheroids with large aspect ratio is the so-called iterative extended boundary condition method (IEBCM) [33].

The main feature of this technique is to represent the internal field by several subregion spherical function expansions centered along the major axis of the prolate spheroid. The contiguous subregional expansions are linked to each other by being matched in the overlapping zones. The set of unknown expanded coefficients of internal field can be determined by using the point-matching method (PMM). It has been reported that in some spheroidal cases, the use of IEBCM instead of the regular EBCM allows to more than quadruple the maximum convergent size parameter. However, because the first step in this procedure is to approximate the highly lossy dielectric object with a perfectly conducting object of the same shape for its initial solution, it is restricted by the conductivities of the dielectric particles and the maximum convergent size parameter of EBCM for such perfectly conducting object. Moreover, as pointed in [34], PMM is less flexible in terms of applications to different particle shapes due to the fact that, the more the particle's geometry departs from that of a sphere, the more unsuitable the expansions of the fields in spherical vector wave functions. Thus, elongated particles require the use of specially adapted PMM implementations with longer computation time and higher computer-code complexity. Another similar technique using PMM to solve scattering from particles enclosed by smooth surfaces is the general multipole technique (GMT), which represents electromagnetic field vectors by multiple spherical expansions about several expansion origins which are located at appropriate positions in the interior region [35]. The GMT has been successfully used for particles with smooth surfaces, such as hemispherically or spherically capped cylinders, yet there are issues when it is used in the scattering computations of finite cylinders with flat ends reported. Recently, null field method with discrete sources (NF-DS) is proposed to deal with the instability of conventional EBCM [36–39]. Its numerical stability is achieved at the expense of considerable increase in computer complexity, and the resolution of this method can be affected by the localization of the sources.

In this paper, we propose a new iterative technique applicable for electromagnetic scattering by finite dielectric cylinders with large aspect ratio. With the understanding that for such cylinders a direct application of the EBCM often leads to numerical instability, the procedure starts by dividing the cylinder into several identical sub-cylinder to reduce the aspect ratio for each part to which the EBCM can be applied. A subtle technical issue arises here: since any two neighboring sub-cylinder are touching via the division interface, the conventional multi-scatterer equation method is not directly applicable because it requires that the circumscribing spheres of the sub-cylinder

exclude each other [40]. Rather, boundary conditions at the division interface need to be satisfied and carefully incorporated into the EBCM formalism. The subtlety lies in the fact that boundary conditions at the division interfaces are point-wise while the EBCM is in an integral form. For such concern, we introduce some intermediate variables that have specific meanings, where the boundary conditions are incorporated. Moreover, since these variables are expressed in terms of surface integrals, the drawbacks of PPM inherent in IEBCM or GMT is avoided. The intercoupling relations of multipole expansions for sub-cylinder are constructed with the help of translational addition theorems and can be solved iteratively. The impact of translational addition theorem on the convergence property of the resulting linear system is also carefully treated in the iterative procedure.

2. T-MATRIX APPROACH

In T-matrix approach, the incident, scattered, and internal fields are expressed in terms of the spherical harmonics, respectively

$$\begin{aligned}
\mathbf{E}^{inc}\left(\bar{r}'\right) &= \sum_{n,m}\left\{a_{mn}^{inc,M} Rg\bar{M}_{mn}\left(\bar{r}'\right) + a_{mn}^{inc,N} Rg\bar{N}_{mn}\left(\bar{r}'\right)\right\} \\
\mathbf{E}^{sca}\left(\bar{r}'\right) &= \sum_{n,m}\left\{a_{mn}^{sca,M} \bar{M}_{mn}\left(\bar{r}'\right) + a_{mn}^{sca,N} \bar{N}_{mn}\left(\bar{r}'\right)\right\} \\
\mathbf{E}^{int}\left(\bar{r}'\right) &= \sum_{n,m}\left\{a_{mn}^{int,M} Rg\bar{M}_{mn}\left(\bar{r}'\right) + a_{mn}^{int,N} Rg\bar{N}_{mn}\left(\bar{r}'\right)\right\}, \qquad (1)
\end{aligned}$$

where $Rg\bar{M}_{mn}$, $Rg\bar{N}_{mn}$, $\bar{M}_{mn}$ and $\bar{N}_{mn}$ are the vector spherical waves respectively as defined in [41]. A list of variables used in this paper is provided at the end of the paper in Table 3 for referential convenience. Owing to the linearity of Maxwell's equations and boundary conditions, the linear relation between the scattered field coefficients $\bar{a}^{sca}$ on one hand and the incident field coefficients $\bar{a}^{inc}$ on the other hand is given by the system transfer operator T as follows [25]:

$$\bar{a}^{sca} = \bar{\bar{T}}\,\bar{a}^{inc}. \qquad (2)$$

Eq. (2) is a cornerstone of the T-matrix formulation. Because the T matrix includes the full information about the wave scattering and absorption properties of a particle at a given wavelength, all quantities of interest in remote sensing, such as the amplitude scattering matrix, the scattering cross section as well as the expansion coefficients of the Stokes scattering matrix can be expressed in terms of the T matrix. This is a important advantage of the T-matrix approach.

The widely utilized scheme for computing the T matrix for simple particles is based on EBCM, which is also called the null field approach. As an alternative to solve the surface integral equation, EBCM assumes an inscribing sphere and a circumscribing sphere with their centers at the origin contained within the scatterer, then applies the extended boundary condition inside the inscribing sphere and outside the circumscribing sphere, respectively. Rather than considering the coupling of the incident and scattered fields directly, the coupling between the incident and internal represented by the RgQ matrix, and scattered and internal fields represented by the Q matrix is explicitly treated. In the EBCM, expressions for matrices RgQ and Q are derived from an integral equation approach which can be found in [41]. Then the T matrix can be easily obtained from the following relation between the RgQ matrix and Q matrix

$$\bar{\bar{T}} = -Rg\bar{\bar{Q}}^t \cdot \left(\bar{\bar{Q}}^t\right)^{-1} \tag{3}$$

where the subscript t represents the transpose of matrix.

An another important advantage of the T-matrix approach is that, unlike many other methods of calculating scattering where the entire calculation needs to be repeated for each new incident field, the T matrix only needs to be calculated once because it is independent of any specific incident field. Moreover, utilizing geometrical symmetries of particles can drastically reduce CPU-time requirements. Therefore, for a scatterer with moderate aspect ratio, T-matrix approach is a very effective technique for scattering computation, especially for calculating the scattering properties of an ensemble of randomly oriented particles. Fig. 1 clearly demonstrates the accuracy of T-matrix approach predictions against experimental benchmarks reported by Allen and McCormick [42], where the parameters of two samples are listed in Table 1 and the imaginary part of dielectric constant is $0.036i$. The maximum diameter and maximum length of the samples are $2a$ and $2c$, respectively.

Table 1. Parameters for the samples.

Sample	①	②
ka	0.305	0.609
c/a	2.500	2.503
$\mathrm{Re}(\epsilon)$	3.16	3.14

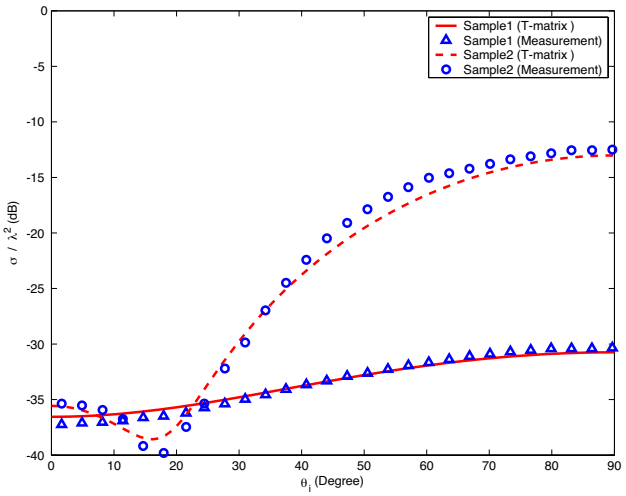

Figure 1. Backscattering cross section comparisons between T-matrix approach and measurements of dielectric cylinders excited by a circularly polarized plane wave.

3. TRANSLATIONAL ADDITION THEOREM

Translational addition theorem is a powerful analytic tool to solve theoretically for the scattering properties of multiple scatterers. Since the early studies of Friedman and Russek [43] in the 1950s, considerable efforts have been devoted to the formulation and evaluation of the scalar addition coefficients.

Consider now coordinate systems i and j having the same spatial orientation and denote by $\bar{r}_{ji}$ the vector pointing to the origin of coordinate system j from the origin of coordinate system i as illustrated in Fig. 2. Specifically, for $\bar{r}_j = \bar{r}_i + \bar{r}_{ji}$, where $(r_j, \theta_j, \varphi_j)$, $(r_i, \theta_i, \varphi_i)$ and $(r_{ji}, \theta_{ji}, \varphi_{ji})$ are their respective spherical coordinates, the scalar translational addition theorem for the solid translation from the coordinate system i to the coordinate system j can be expressed as:

$$\psi_{mn}(r_j, \theta_j, \varphi_j) = \sum_{\mu,\nu} \psi_{\mu\nu}(r_i, \theta_i, \varphi_i) C_{\mu\nu}^{mn}(r_{ji}, \theta_{ji}, \varphi_{ji}), \tag{4}$$

where the scalar wave function is

$$\psi_{mn}(r, \theta, \phi) = P_n^m(\cos\theta) z_n(kr) e^{im\phi}. \tag{5}$$

Here a time dependence of $e^{-i\omega t}$ is assumed and P_n^m is the associated Legendre function. z_n is appropiately selected between the following

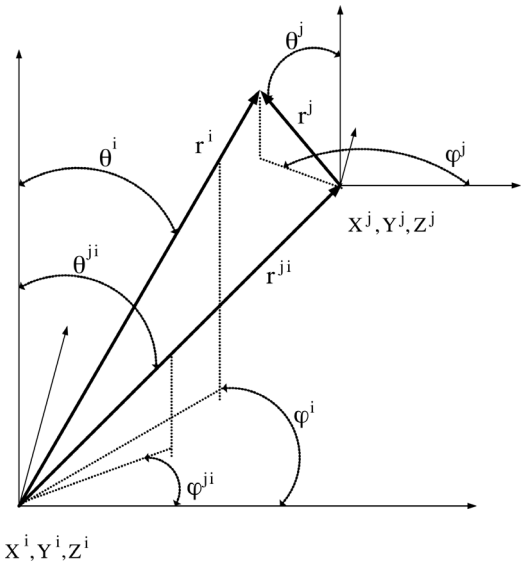

Figure 2. Translation of coordinates from origin i to origin j.

two functions: the spherical Bessel function of the first kind j_n or the spherical Hankel function of the first kind $h_n^{(1)}$. The scalar translational coefficient is given as [43, 44]

$$C_{\mu\nu}^{mn}(r_{ji},\theta_{ji},\phi_{ji}) = (-1)^m i^{(\nu-n)}(2\nu+1)\sum_p i^p a(m,n,-\mu,\nu,p) \times P_p^{m-\mu}(\cos\theta_{ji}) z_p(kr_{ji}) e^{i(m-\mu)\phi_{ji}} \quad (6)$$

where $a(m,n,\mu,\nu,p)$ is the Gaunt coefficient, which was first introduced by Gaunt [45] in his study of the atomic structure of helium triplets. In 1971, Bruning and Lo [46] derived a recursive scheme to calculate the Gaunt coefficients for the vector addition theorem efficiently for a special case of bi-sphere scattering problem in which the translation was along the z axis. However, the calculation of the required number of Gaunt coefficients represents a tremendous expenditure of effort when the truncation number is large. An alternative is the recursive approach devised by Mackowski [47]. By utilizing the recurrence relations for the scalar translational addition coefficients [48] and the starting expression $C_{\mu\nu}^{00}$, the scalar addition coefficients can be obtained for all values of m, n, μ and ν.

For the case of vector spherical wave functions, the vector addition

theorems have the form

$$\begin{bmatrix} Rg\bar{M}_{mn}(\bar{r}_j) \\ Rg\bar{N}_{mn}(\bar{r}_j) \end{bmatrix} = \sum_{\mu,\nu} \left\{ \begin{bmatrix} RgA^{mn}_{\mu\nu}(\bar{r}_{ji}) \\ RgB^{mn}_{\mu\nu}(\bar{r}_{ji}) \end{bmatrix} Rg\bar{M}_{\mu\nu}(\bar{r}_i) + \begin{bmatrix} RgB^{mn}_{\mu\nu}(\bar{r}_{ji}) \\ RgA^{mn}_{\mu\nu}(\bar{r}_{ji}) \end{bmatrix} Rg\bar{N}_{\mu\nu}(\bar{r}_i) \right\} \tag{7}$$

and

$$\begin{bmatrix} \bar{M}_{mn}(\bar{r}_j) \\ \bar{N}_{mn}(\bar{r}_j) \end{bmatrix} = \sum_{\mu,\nu} \left\{ \begin{bmatrix} A^{mn}_{\mu\nu}(\bar{r}_{ji}) \\ B^{mn}_{\mu\nu}(\bar{r}_{ji}) \end{bmatrix} Rg\bar{M}_{\mu\nu}(\bar{r}_i) + \begin{bmatrix} B^{mn}_{\mu\nu}(\bar{r}_{ji}) \\ A^{mn}_{\mu\nu}(\bar{r}_{ji}) \end{bmatrix} Rg\bar{N}_{\mu\nu}(\bar{r}_i) \right\} \tag{8}$$

for the condition $\bar{r}_i < \bar{r}_{ji}$, where the vector spherical waves with and without the prefix Rg stand for regular and outgoing waves, respectively.

Cruzan formulated the vector translation coefficients using the Wigner $3j$ symbols [49] as

$$\begin{aligned} A^{mn}_{\mu\nu} &= (-1)^{\mu}\, i^{\nu-n} \frac{2\nu+1}{2\nu(\nu+1)} \sum_p i^p [\nu(\nu+1) + n(n+1) - p(p+1)] \\ &\quad \times a\,(m,n,-\mu,\nu,p)\, z_p\,(kr_{ji})\, P_p^{m-\mu}(\cos\theta_{ji}) \exp[i(m-\mu)\phi_{ji}] \\ B^{mn}_{\mu\nu} &= (-1)^{\mu+1}\, i^{\nu-n} \frac{2\nu+1}{2\nu(\nu+1)} \\ &\quad \times \sum_p i^p \sqrt{[p^2-(n+\nu)^2][(n+\nu+1)^2-p^2]} \\ &\quad \times a(m,n,-\mu,\nu,p,p-1) z_p(kr_{ji}) \\ &\quad \times P_p^{m-\mu}(\cos\theta_{ji}) \exp[i(m-\mu)\phi_{ji}], \end{aligned} \tag{9}$$

where

$$\begin{aligned} a(m,n,-m,\nu,p,p-1) &= (2p+1) \left[\frac{(n+m)!(\nu-m)!}{(n-m)!(\nu+m)!} \right]^{1/2} \\ &\quad \times \begin{pmatrix} n & \nu & p \\ m & \mu & 0 \end{pmatrix} \begin{pmatrix} n & \nu & p-1 \\ 0 & 0 & 0 \end{pmatrix}. \end{aligned} \tag{10}$$

Later Tsang and Kong [50] reported a sign error in Cruzan's translation formulas.

In addition, both Stein [44] and Mackowski [47] expressed the vector translational addition coefficients in terms of seven and six scalar translational addition coefficients, respectively. In fact, as Mackowski pointed out, these two formulations can be converted to each other [47]. The expressions by Mackowski are given by

$$A_{\mu\nu}^{mn} = \frac{\begin{array}{l}(\nu-\mu)(\nu+\mu+1)C_{\mu+1\nu}^{m+1n} \\ +2\mu m C_{\mu\nu}^{mn} + (n+m)(n-m+1)C_{\mu-1\nu}^{m-1n}\end{array}}{2\nu(\nu+1)}$$

$$B_{\mu\nu}^{mn} = \frac{i(2\nu+1)}{2\nu(\nu+1)(2\nu+3)}\Big[(\nu+\mu+1)(\nu+\mu+2)C_{\mu+1\nu+1}^{m+1n} - 2m(\nu+\mu+1)C_{\mu\nu+1}^{mn} - (n+m)(n-m+1)C_{\mu-1\nu+1}^{m-1n}\Big]. \quad (11)$$

It follows that this set of equations do not need geometrical information of the volumes. This makes Mackowski's formulations more convenient in practical computations, and we choose to use these formulations in our paper.

4. PROPOSED METHOD

Consider a dielectric cylinder with large aspect ratio. We use $N-1$ hypothetic surfaces to divide it into a cluster of N identical sub-cylinder, for each the T matrix can be directly calculated by using the conventional EBCM. The simple case of two sub-cylinder division is depicted in Fig. 3. Such case will serve as the basis of our analysis, since the extension to an N sub-cylinder case is straightforward. Now that these two sub-cylinder are touching via the division interface,

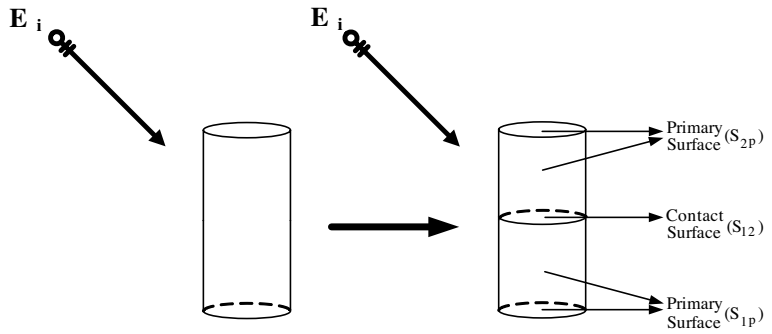

Figure 3. Division of a cylinder into two identical sub-cylinder.

a subtle technical issue arises here: the conventional multi-scatterer equation method is not directly applicable because it requires that the circumscribing spheres of the sub-cylinder exclude each other [40]. It is necessary that boundary conditions at the division interface be satisfied and carefully incorporated into the EBCM formalism. The subtlety lies in the fact that boundary conditions at the division interface are point-wise while the EBCM is in an integral form. For such concern, we shall introduce some intermediate variables that have specific meanings, where the boundary conditions are incorporated.

Since the EBCM involves surface integrals and since cylinder division generates hypothetical interfaces, before we proceed we need to denote these surfaces carefully. Each sub-cylinder will contain a primary surface and an interface. We shall start number ordering from the lowest sub-cylinder (see Fig. 3). The primary surface of sub-cylinder 1, S_{1p}, includes its cylindrical surface and the lower surface, while that of sub-cylinder 2, S_{2p}, includes its cylindrical surface and the upper surface. The common interface is denoted by S_{12}. The center of sub-cylinder 1 is $\overline{r}_1$ and that of sub-cylinder 2 is $\overline{r}_2$. Utilizing T matrix, the expanded coefficients $\bar{a}_{mn}$ and $\bar{a}^s_{mn}$ for each part are related as follows

$$\begin{aligned}
\begin{bmatrix} a_{mn}^{s(M)(1)p} \\ a_{mn}^{s(N)(1)p} \end{bmatrix} + \begin{bmatrix} a_{mn}^{s(M)(1)u} \\ a_{mn}^{s(N)(1)u} \end{bmatrix} &= \bar{\bar{T}} \cdot \left\{ \begin{bmatrix} a_{mn}^{(M)(1)p} \\ a_{mn}^{(N)(1)p} \end{bmatrix} + \begin{bmatrix} a_{mn}^{(M)(1)u} \\ a_{mn}^{(N)(1)u} \end{bmatrix} \right\} \\
\begin{bmatrix} a_{mn}^{s(M)(2)p} \\ a_{mn}^{s(N)(2)p} \end{bmatrix} + \begin{bmatrix} a_{mn}^{s(M)(2)d} \\ a_{mn}^{s(N)(2)d} \end{bmatrix} &= \bar{\bar{T}} \cdot \left\{ \begin{bmatrix} a_{mn}^{(M)(2)p} \\ a_{mn}^{(N)(2)p} \end{bmatrix} + \begin{bmatrix} a_{mn}^{(M)(2)d} \\ a_{mn}^{(N)(2)d} \end{bmatrix} \right\}. \quad (12)
\end{aligned}$$

Now for fields expanded in terms of vector spherical waves with different origins, we introduce the following intermediate variables:

$$\begin{aligned}
\begin{bmatrix} a_{mn}^{(M)(1)p} \\ a_{mn}^{(N)(1)p} \end{bmatrix} &= -ik(-1)^m \int_{S_{1p}} dS \Bigg\{ i\omega\mu\hat{n}_1 \times \mathbf{H}_1(\mathbf{r}) \cdot \begin{bmatrix} \bar{M}_{-mn}(\overline{rr}_1) \\ \bar{N}_{-mn}(\overline{rr}_1) \end{bmatrix} \\
&\quad + k\hat{n}_1 \times \mathbf{E}_1(\mathbf{r}) \cdot \begin{bmatrix} \bar{N}_{-mn}(\overline{rr}_1) \\ \bar{M}_{-mn}(\overline{rr}_1) \end{bmatrix} \Bigg\} \quad (13) \\
\begin{bmatrix} a_{mn}^{(M)(2)p} \\ a_{mn}^{(N)(2)p} \end{bmatrix} &= -ik(-1)^m \int_{S_{2p}} dS \Bigg\{ i\omega\mu\hat{n}_2 \times \mathbf{H}_2(\mathbf{r}) \cdot \begin{bmatrix} \bar{M}_{-mn}(\overline{rr}_2) \\ \bar{N}_{-mn}(\overline{rr}_2) \end{bmatrix} \\
&\quad + k\hat{n}_2 \times \mathbf{E}_2(\mathbf{r}) \cdot \begin{bmatrix} \bar{N}_{-mn}(\overline{rr}_2) \\ \bar{M}_{-mn}(\overline{rr}_2) \end{bmatrix} \Bigg\} \quad (14)
\end{aligned}$$

$$\begin{bmatrix} a_{mn}^{s(M)(1)p} \\ a_{mn}^{s(N)(1)p} \end{bmatrix} = ik(-1)^m \int\limits_{S_{1p}} dS \Bigg\{ i\omega\mu\hat{n}_1 \times \mathbf{H}_1(\mathbf{r}) \cdot \begin{bmatrix} Rg\bar{M}_{-mn}(\overline{rr}_1) \\ Rg\bar{N}_{-mn}(\overline{rr}_1) \end{bmatrix} + k\hat{n}_1 \times \mathbf{E}_1(\mathbf{r}) \cdot \begin{bmatrix} Rg\bar{N}_{-mn}(\overline{rr}_1) \\ Rg\bar{M}_{-mn}(\overline{rr}_1) \end{bmatrix} \Bigg\} \tag{15}$$

$$\begin{bmatrix} a_{mn}^{s(M)(2)p} \\ a_{mn}^{s(N)(2)p} \end{bmatrix} = ik(-1)^m \int\limits_{S_{2p}} dS \Bigg\{ i\omega\mu\hat{n}_2 \times \mathbf{H}_2(\mathbf{r}) \cdot \begin{bmatrix} Rg\bar{M}_{-mn}(\overline{rr}_2) \\ Rg\bar{N}_{-mn}(\overline{rr}_2) \end{bmatrix} + k\hat{n}_2 \times \mathbf{E}_2(\mathbf{r}) \cdot \begin{bmatrix} Rg\bar{N}_{-mn}(\overline{rr}_2) \\ Rg\bar{M}_{-mn}(\overline{rr}_2) \end{bmatrix} \Bigg\} \tag{16}$$

where the superscript p denotes the primary part, and s the scattered field. These intermediate variables are not arbitrary quantities but have specific physical meanings. They represent the expansion coefficients of the exciting fields and scattered fields due to the primary surfaces of these two sub-cylinder, respectively. Similarly, the respective expansion coefficients of the exciting fields and scattered fields due to the interface of these two sub-cylinder are

$$\begin{bmatrix} a_{mn}^{(M)(1)u} \\ a_{mn}^{(N)(1)u} \end{bmatrix} = -ik(-1)^m \int\limits_{S_{12}} dS \Bigg\{ i\omega\mu\hat{n}_1 \times \mathbf{H}_1(\mathbf{r}) \cdot \begin{bmatrix} \bar{M}_{-mn}(\overline{rr}_1) \\ \bar{N}_{-mn}(\overline{rr}_1) \end{bmatrix} + k\hat{n}_1 \times \mathbf{E}_1(\mathbf{r}) \cdot \begin{bmatrix} \bar{N}_{-mn}(\overline{rr}_1) \\ \bar{M}_{-mn}(\overline{rr}_1) \end{bmatrix} \Bigg\} \tag{17}$$

$$\begin{bmatrix} a_{mn}^{(M)(2)d} \\ a_{mn}^{(N)(2)d} \end{bmatrix} = -ik(-1)^m \int\limits_{S_{12}} dS \Bigg\{ i\omega\mu\hat{n}_2 \times \mathbf{H}_2(\mathbf{r}) \cdot \begin{bmatrix} \bar{M}_{-mn}(\overline{rr}_2) \\ \bar{N}_{-mn}(\overline{rr}_2) \end{bmatrix} + k\hat{n}_2 \times \mathbf{E}_2(\mathbf{r}) \cdot \begin{bmatrix} \bar{N}_{-mn}(\overline{rr}_2) \\ \bar{M}_{-mn}(\overline{rr}_2) \end{bmatrix} \Bigg\} \tag{18}$$

$$\begin{bmatrix} a_{mn}^{s(M)(1)u} \\ a_{mn}^{s(N)(1)u} \end{bmatrix} = ik(-1)^m \int\limits_{S_{12}} dS \Bigg\{ i\omega\mu\hat{n}_1 \times \mathbf{H}_1(\mathbf{r}) \cdot \begin{bmatrix} Rg\bar{M}_{-mn}(\overline{rr}_1) \\ Rg\bar{N}_{-mn}(\overline{rr}_1) \end{bmatrix} + k\hat{n}_1 \times \mathbf{E}_1(\mathbf{r}) \cdot \begin{bmatrix} Rg\bar{N}_{-mn}(\overline{rr}_1) \\ Rg\bar{M}_{-mn}(\overline{rr}_1) \end{bmatrix} \Bigg\} \tag{19}$$

$$\begin{bmatrix} a_{mn}^{s(M)(2)d} \\ a_{mn}^{s(N)(2)d} \end{bmatrix} = ik(-1)^m \int\limits_{S_{12}} dS \Bigg\{ i\omega\mu\hat{n}_2 \times \mathbf{H}_2(\mathbf{r}) \cdot \begin{bmatrix} Rg\bar{M}_{-mn}(\overline{rr}_2) \\ Rg\bar{N}_{-mn}(\overline{rr}_2) \end{bmatrix} + k\hat{n}_2 \times \mathbf{E}_2(\mathbf{r}) \cdot \begin{bmatrix} Rg\bar{N}_{-mn}(\overline{rr}_2) \\ Rg\bar{M}_{-mn}(\overline{rr}_2) \end{bmatrix} \Bigg\}. \tag{20}$$

In the above, $\hat{n}_i$ is the outward pointing unit normal vectors on the surface S_i of sub-cylinder i. We have $\hat{n}_2 = -\hat{n}_1$ on the surface S_{12}.

Since the terms $\bar{a}_{mn}^{(1)u}$ and $\bar{a}_{mn}^{s(2)d}$ are expressed in terms of the tangential fields on the interface, it is natural to relate them in some way. Yet since each involves vector spherical waves with different origins, a transformation of origin must first be performed using the translational addition theorem. For the latter task we have the convenience of reducing the double summation over m and ν to single summation over ν because the translation is along the z axis. Shifting the origin from $\overline{r}_1$ to $\overline{r}_2$, the term $\bar{a}_{mn}^{(1)u}$ can thus be expressed as

$$
\begin{aligned}
&\begin{bmatrix} a_{mn}^{(M)(1)u} \\ a_{mn}^{(N)(1)u} \end{bmatrix} = -ik\,(-1)^m \int\limits_{S_{1,u}} dS i\omega\mu\hat{n}_1 \times \mathbf{H}_1\,(\mathbf{r}) \\
&\cdot \begin{bmatrix} \sum\limits_{\nu} \left\{ A_{-m\nu}^{-mn}(\overline{r_1 r}_2) Rg\bar{M}_{-m\nu}(\overline{rr}_2) + B_{-m\nu}^{-mn}(\overline{r_1 r}_2) Rg\bar{N}_{-m\nu}(\overline{rr}_2) \right\} \\ \sum\limits_{\nu} \left\{ A_{-m\nu}^{-mn}(\overline{r_1 r}_2) Rg\bar{N}_{-m\nu}(\overline{rr}_2) + B_{-m\nu}^{-mn}(\overline{r_1 r}_2) Rg\bar{M}_{-m\nu}(\overline{rr}_2) \right\} \end{bmatrix} \\
&-ik(-1)^m \int\limits_{S_{1,u}} dSk\hat{n}_1 \times \mathbf{E}_1(\mathbf{r}) \\
&\cdot \begin{bmatrix} \sum\limits_{\nu} \left\{ A_{-m\nu}^{-mn}(\overline{r_1 r}_2) Rg\bar{N}_{-m\nu}(\overline{rr}_2) + B_{-m\nu}^{-mn}(\overline{r_1 r}_2) Rg\bar{M}_{-m\nu}(\overline{rr}_2) \right\} \\ \sum\limits_{\nu} \left\{ A_{-m\nu}^{-mn}(\overline{r_1 r}_2) Rg\bar{M}_{-m\nu}(\overline{rr}_2) + B_{-m\nu}^{-mn}(\overline{r_1 r}_2) Rg\bar{N}_{-m\nu}(\overline{rr}_2) \right\} \end{bmatrix} \\
&= \sum_{\nu} A_{-m\nu}^{-mn}(\overline{r_1 r}_2) ik(-1)^m \int\limits_{S_{2,d}} dS i\omega\mu\hat{n}_2 \times \mathbf{H}_2(\mathbf{r}) \cdot \begin{bmatrix} Rg\bar{M}_{-mn}(\overline{rr}_2) \\ Rg\bar{N}_{-mn}(\overline{rr}_2) \end{bmatrix} \\
&+k\hat{n}_2 \times \mathbf{E}_2(\mathbf{r}) \cdot \begin{bmatrix} Rg\bar{N}_{-mn}(\overline{rr}_2) \\ Rg\bar{M}_{-mn}(\overline{rr}_2) \end{bmatrix} \\
&+ \sum_{v} B_{-m\nu}^{-mn}(\overline{r_1 r}_2) ik(-1)^m \int\limits_{S_{2,d}} dS i\omega\mu\hat{n}_2 \times \mathbf{H}_2(\mathbf{r}) \cdot \begin{bmatrix} Rg\bar{N}_{-mn}(\overline{rr}_2) \\ Rg\bar{M}_{-mn}(\overline{rr}_2) \end{bmatrix} \\
&+k\hat{n}_2 \times \mathbf{E}_2(\mathbf{r}) \cdot \begin{bmatrix} Rg\bar{M}_{-mn}(\overline{rr}_2) \\ Rg\bar{N}_{-mn}(\overline{rr}_2) \end{bmatrix}. \qquad (21)
\end{aligned}
$$

In the second equality of the above equation, we specifically make use of the boundary conditions

$$\hat{n}_1 \times \mathbf{H}_1 = -\hat{n}_2 \times \mathbf{H}_2, \quad \hat{n}_1 \times \mathbf{E}_1 = -\hat{n}_2 \times \mathbf{E}_2. \qquad (22)$$

The intermediate variables of the second sub-cylinder (20) allow us to

further express (21) as

$$\begin{bmatrix} a_{mn}^{(M)(1)u} \\ a_{mn}^{(N)(1)u} \end{bmatrix} = \sum_{\nu} A_{-mn}^{-m\nu}(\overline{r_1 r_2}) \begin{bmatrix} a_{mv}^{s(M)(2)d} \\ a_{mv}^{s(N)(2)d} \end{bmatrix} + \sum_{\nu} B_{-mn}^{-m\nu}(\overline{r_1 r_2}) \begin{bmatrix} a_{mv}^{s(N)(2)d} \\ a_{mv}^{s(M)(2)d} \end{bmatrix}. \quad (23)$$

Note that for a single scatterer, the incident field is equal to the exciting field. In our case, the virtual partition shall not change this property. Now if we let the global origin coincidence with $\overline{r}_1$, we have

$$\begin{aligned} \begin{bmatrix} a_{mn}^{(M)} \\ a_{mn}^{(N)} \end{bmatrix} = & -ik(-1)^m \int\limits_{S_{1,p}} dS i\omega\mu \hat{n}_1 \times \mathbf{H}_1(\mathbf{r}) \cdot \begin{bmatrix} \bar{M}_{-mn}(\overline{rr}_1) \\ \bar{N}_{-mn}(\overline{rr}_1) \end{bmatrix} \\ & + k\hat{n}_1 \times \mathbf{E}_1(\mathbf{r}) \cdot \begin{bmatrix} \bar{N}_{-mn}(\overline{rr}_1) \\ \bar{M}_{-mn}(\overline{rr}_1) \end{bmatrix} \\ & - ik(-1)^m \int\limits_{S_{2,p}} dS i\omega\mu \hat{n}_2 \times \mathbf{H}_2(\mathbf{r}) \cdot \begin{bmatrix} \bar{M}_{-mn}(\overline{rr}_1) \\ \bar{N}_{-mn}(\overline{rr}_1) \end{bmatrix} \\ & + k\hat{n}_2 \times \mathbf{E}_2(\mathbf{r}) \cdot \begin{bmatrix} \bar{N}_{-mn}(\overline{rr}_1) \\ \bar{M}_{-mn}(\overline{rr}_1) \end{bmatrix}. \end{aligned} \quad (24)$$

By applying transformation of origin on the vector spherical waves in the second surface integral, and making use of the intermediate variables (16), we obtain

$$\begin{bmatrix} a_{mn}^{(M)} \\ a_{mn}^{(N)} \end{bmatrix} = \begin{bmatrix} a_{mn}^{(M)(1)p} \\ a_{mn}^{(N)(1)p} \end{bmatrix} - \sum_{\nu} A_{-m\nu}^{-mn}(\overline{r_1 r}_2) \begin{bmatrix} a_{m\nu}^{s(M)(2)p} \\ a_{m\nu}^{s(N)(2)p} \end{bmatrix} - \sum_{\nu} B_{-m\nu}^{-mn}(\overline{r_1 r}_2) \begin{bmatrix} a_{m\nu}^{s(N)(2)p} \\ a_{m\nu}^{s(M)(2)p} \end{bmatrix}. \quad (25)$$

Combining (23) and (25), and using variable substitution, yields

$$\begin{bmatrix} a_{mn}^{(M)} \\ a_{mn}^{(N)} \end{bmatrix} = \begin{bmatrix} a_{mn}^{(M)(1)} \\ a_{mn}^{(N)(1)} \end{bmatrix} - \sum_{\nu} A_{-m\nu}^{-mn}(\overline{r_1 r}_2) \begin{bmatrix} a_{m\nu}^{s(M)(2)} \\ a_{m\nu}^{s(N)(2)} \end{bmatrix} - \sum_{\nu} B_{-m\nu}^{-mn}(\overline{r_1 r}_2) \begin{bmatrix} a_{m\nu}^{s(N)(2)} \\ a_{m\nu}^{s(M)(2)} \end{bmatrix} \quad (26)$$

where

$$a_{mn}^{(M)(1)} = a_{mn}^{(M)(1)u} + a_{mn}^{(M)(1)p} \tag{27}$$
$$a_{mn}^{(N)(1)} = a_{mn}^{(N)(1)u} + a_{mn}^{(N)(1)p} \tag{28}$$
$$a_{mn}^{s(M)(2)} = a_{mn}^{s(M)(2)d} + a_{mn}^{s(M)(2)p} \tag{29}$$
$$a_{mn}^{s(N)(2)} = a_{mn}^{s(N)(2)d} + a_{mn}^{s(N)(2)p}. \tag{30}$$

Similarly, we can also establish the following system of equations by focusing on the upper part of cylinder as follows

$$\begin{bmatrix} a_{mn}^{(M)\prime} \\ a_{mn}^{(N)\prime} \end{bmatrix} = \begin{bmatrix} a_{mn}^{(M)(2)} \\ a_{mn}^{(N)(2)} \end{bmatrix} - \sum_{\nu} A_{-m\nu}^{-mn}(\overline{r_2 r}_1) \begin{bmatrix} a_{m\nu}^{s(M)(1)} \\ a_{m\nu}^{s(N)(1)} \end{bmatrix} - \sum_{\nu} B_{-m\nu}^{-mn}(\overline{r_2 r}_1) \begin{bmatrix} a_{m\nu}^{s(N)(1)} \\ a_{m\nu}^{s(M)(1)} \end{bmatrix}, \tag{31}$$

where the multipole coefficients of the incident plane wave $a_{mn}^{(M)\prime}$ and $a_{mn}^{(N)\prime}$ differ from $a_{mn}^{(M)}$ and $a_{mn}^{(N)}$ by a factor $e^{ikhcos\theta_i}$. Here h is the height of each sub-cylinder.

The scattered field can be treated similarly. Applying the translational addition theorems (7) to the (19) and the following equation, respectively,

$$\begin{aligned} \begin{bmatrix} a_{mn}^{s(M)} \\ a_{mn}^{s(N)} \end{bmatrix} &= ik(-1)^m \int_S dS \Bigg\{ i\omega\mu\hat{n} \times \mathbf{H}(\mathbf{r}) \cdot \begin{bmatrix} Rg\bar{M}_{-mn}(\overline{rr}_1) \\ Rg\bar{N}_{-mn}(\overline{rr}_1) \end{bmatrix} \\ &\quad + k\hat{n} \times \mathbf{E}(\mathbf{r}) \cdot \begin{bmatrix} Rg\bar{N}_{-mn}(\overline{rr}_1) \\ Rg\bar{M}_{-mn}(\overline{rr}_1) \end{bmatrix} \Bigg\} \\ &= ik(-1)^m \int_{S_{1,p}} dS \Bigg\{ i\omega\mu\hat{n}_1 \times \mathbf{H}_1(\mathbf{r}) \cdot \begin{bmatrix} Rg\bar{M}_{-mn}(\overline{rr}_1) \\ Rg\bar{N}_{-mn}(\overline{rr}_1) \end{bmatrix} \\ &\quad + k\hat{n}_1 \times \mathbf{E}_1(\mathbf{r}) \cdot \begin{bmatrix} Rg\bar{N}_{-mn}(\overline{rr}_1) \\ Rg\bar{M}_{-mn}(\overline{rr}_1) \end{bmatrix} \Bigg\} \\ &+ ik(-1)^m \int_{S_{2,p}} dS \Bigg\{ i\omega\mu\hat{n}_2 \times \mathbf{H}_2(\mathbf{r}) \cdot \begin{bmatrix} Rg\bar{M}_{-mn}(\overline{rr}_1) \\ Rg\bar{N}_{-mn}(\overline{rr}_1) \end{bmatrix} \\ &\quad + k\hat{n}_2 \times \mathbf{E}_2(\mathbf{r}) \cdot \begin{bmatrix} Rg\bar{N}_{-mn}(\overline{rr}_1) \\ Rg\bar{M}_{-mn}(\overline{rr}_1) \end{bmatrix} \Bigg\} \end{aligned} \tag{32}$$

we can easily derive the following equations

$$\begin{bmatrix} a_{mn}^{s(M)(1)u} \\ a_{mn}^{s(N)(1)u} \end{bmatrix} = -\sum_{\nu} RgA_{-m\nu}^{-mn}(\overline{r_1 r}_2) \begin{bmatrix} a_{mn}^{s(M)(2)d} \\ a_{mn}^{s(N)(2)d} \end{bmatrix} - \sum_{\nu} RgB_{-m\nu}^{-mn}(\overline{r_1 r}_2) \begin{bmatrix} a_{m\nu}^{s(N)(2)d} \\ a_{m\nu}^{s(M)(2)d} \end{bmatrix} \tag{33}$$

and

$$\begin{bmatrix} a_{mn}^{s(M)} \\ a_{mn}^{s(N)} \end{bmatrix} = \begin{bmatrix} a_{mn}^{s(M)(1)p} \\ a_{mn}^{s(N)(1)p} \end{bmatrix} + \sum_{\nu} RgA_{-m\nu}^{-mn}(\overline{r_1 r}_2) \begin{bmatrix} a_{m\nu}^{s(M)(2)p} \\ a_{m\nu}^{s(N)(2)p} \end{bmatrix} + \sum_{\nu} RgB_{-m\nu}^{-mn}(\overline{r_1 r}_2) \begin{bmatrix} a_{m\nu}^{s(N)(2)p} \\ a_{m\nu}^{s(M)(2)p} \end{bmatrix}. \tag{34}$$

Combining the above two equations allows us to express the total scattered coefficients of whole cylinder in the primary coordinate system as

$$\begin{bmatrix} a_{mn}^{s(M)} \\ a_{mn}^{s(N)} \end{bmatrix} = \begin{bmatrix} a_{mn}^{s(M)(1)} \\ a_{mn}^{s(N)(1)} \end{bmatrix} + \sum_{\nu} RgA_{-m\nu}^{-mn}(\overline{r_1 r}_2) \begin{bmatrix} a_{m\nu}^{s(M)(2)} \\ a_{m\nu}^{s(N)(2)} \end{bmatrix} + \sum_{\nu} RgB_{-m\nu}^{-mn}(\overline{r_1 r}_2) \begin{bmatrix} a_{m\nu}^{s(N)(2)} \\ a_{m\nu}^{s(M)(2)} \end{bmatrix}. \tag{35}$$

It is clear that the solutions of these coupled, linear, simultaneous equations can be easily obtained by iterative method. The iteration procedure is summarized as follows: Starting with the initial solutions $a_{mn}^{s(M),2} = a_{mn}^{s(N),2} = 0$. From (26) and by using T matrix we obtain the new values of the scattering coefficients $\bar{a}_{mn}^{s,1}$ in (31). In a similar manner, we next use the new values to obtain the scattering coefficients $\bar{a}_{mn}^{s,2}$ in (26). The procedure is repeated until all the coefficients converge.

For the specific case of far zone, the expansion coefficients of the total scattered field can be simply expressed as

$$\begin{bmatrix} a_{mn}^{s(M)total} \\ a_{mn}^{s(N)total} \end{bmatrix} = \begin{bmatrix} a_{mn}^{s(M)(1)} \\ a_{mn}^{s(N)(1)} \end{bmatrix} + \begin{bmatrix} a_{mn}^{s(M)(2)} \\ a_{mn}^{s(N)(2)} \end{bmatrix} \cdot e^{-ikh\cos\theta_s} \tag{36}$$

If we are to use the widely used amplitude scattering matrix $F_{pq}(\hat{k}_s, \hat{k}_i)$ to describe the relation between the amplitudes of the incident and

the scattered fields and represent general properties of the scatterer, its expression is given by

$$F_{qp}(\hat{k}_s, \hat{k}_i) = \sum_{m,n} \left\{ \hat{q} \cdot a_{mn}^{s(M)total} \bar{M}_{mn}(kr, \theta, \phi) + \hat{q} \cdot a_{mn}^{s(N)total} \bar{N}_{mn}(kr, \theta, \phi) \right\} \cdot \hat{p} \quad (37)$$

where $\hat{p}$ and $\hat{q}$ are unit polarizations for the incident and scattered wave, respectively. The expressions of far-field solutions for the outgoing vector spherical waves can be found in [41].

5. ERROR ANALYSIS

In the implementation of our proposed approach, since it involves both T matrix and translational addition theorem, and since it is well known that there are truncation errors and/or other types of errors associated with these two aspects, it is expected that any version of implementation will bear the impact of these errors to varying degree, depending on the nature of the problem at hand and the specifics of the implementation. In the following we shall discuss these issues in turn.

For T matrix computations, theoretically the multipole expansions are of infinite length and the T matrix is of infinite size. However in practical calculations, the summation over m and n has to be truncated, thus a special procedure should be used to check the convergence of the resulting solution over the size of T matrix $N_{\max}$. For axially symmetric scatterers, the T matrix can be decomposed into separate submatrices corresponding to different azimuthal modes m which are independently calculated. For a desired absolute accuracy of computing the expansion coefficients Δ ($\Delta = 10^{-4}$), the following simple convergence criterion can be used to determine $N_{\max}$ [52]

$$\max\left[\left|\frac{c_1(N_{\max}) - c_1(N_{\max}-1)}{c_1(N_{\max})}\right|, \left|\frac{c_2(N_{\max}) - c_2(N_{\max}-1)}{c_2(N_{\max})}\right|\right] \leq \Delta, \quad (38)$$

where

$$c_1(N_{\max}) = -\frac{2\pi}{k^2}\mathrm{Re}\sum_{n=1}^{N_{\max}}(2n+1)\left(T_{0n0n}^{11} + T_{0n0n}^{22}\right) \quad (39)$$

$$c_2(N_{\max}) = \frac{2\pi}{k^2}\sum_{n=1}^{N_{\max}}(2n+1)\left[\left|T_{0n0n}^{11}\right|^2 + \left|T_{0n0n}^{22}\right|^2\right] \quad (40)$$

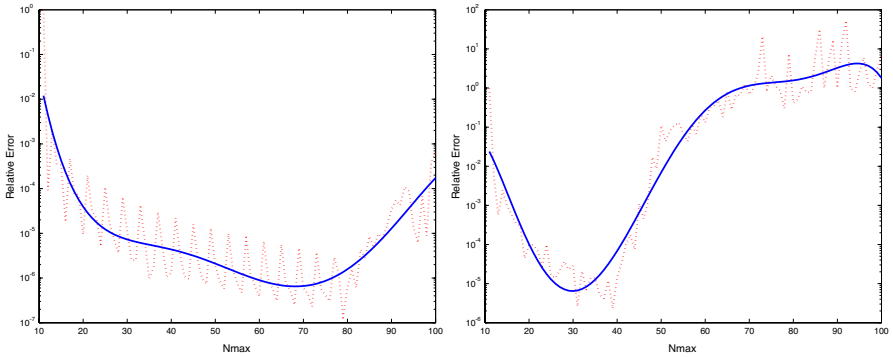

(a) ρ = 1

(b) ρ = 1 / 2

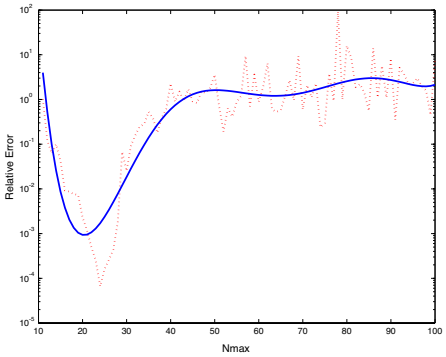

(c) ρ = 1 / 4

Figure 4. Relative errors of the cylindrical cases, where r_v is 5.

In Fig. 4, we plot the relative errors represented by the left side of (38) for three cylindrical cases, where the equal-volume sphere radius r_v is identically set to 5, and the ratio of the horizontal to rotational axes ρ changes from 1 to 0.25. In this figure we clearly see that the relative errors do not monotonically decrease with increasing $N_{\max}$; rather, they demonstrate oscillating behaviors. Such behaviors indicate the need to be very careful and specific when determining $N_{\max}$ in applying T-matrix approach.

For numerical computation of the translational addition coefficients, the order of dipole moment has to be truncated as well which results in truncation error. In a truncation error analysis for the scalar spherical addition theorem [51], it was found that the truncation error decreases as the truncation order $V_{\max}$ increases. Yet in the present analysis, things become more complicated in that the truncation opera-

tions in applying addition theorem and in applying T-matrix approach are convoluted; specifically, the truncation order $V_{\max}$ in applying addition theorem cannot be larger than $N_{\max}$ in applying T-matrix approach. Such constraint may lead to truncation errors that would not show if these two operations were independent.

In order to examine the relative error behavior, we shall compare several cases with different translational scenarios, where various translational distances r_{ji} are used and r_i is identically set to 1. We consider the term $\bar{M}_{1,5}(\bar{r}_j)$ which is approximated by

$$\bar{M}_{1,5}(\bar{r}_j) = \sum_{n=1}^{N_{\max}} \left\{ A_{1,n}^{1,5}(\bar{r}_{ji}) \, Rg\bar{M}_{1,n}(\bar{r}_i) + B_{1,n}^{1,5}(\bar{r}_{ji}) \, Rg\bar{N}_{1,n}(\bar{r}_i) \right\}. \tag{41}$$

Relative error values of $\bar{M}_{1,5}(\bar{r}_j)$ are shown in Fig. 5. As shown in this figure, the relative error can be appreciable when insufficient orders are used in applying the addition theorem. We can make following observations: 1) the relative error decreases when the translational distance increases; 2) the spherical waves of higher order n requires larger expansion orders; 3) the convergence can be improved when the expansion orders increase (from 5 to 35 in this case). Similar observations can be made from Fig. 6, where r_i is identically set to 3.

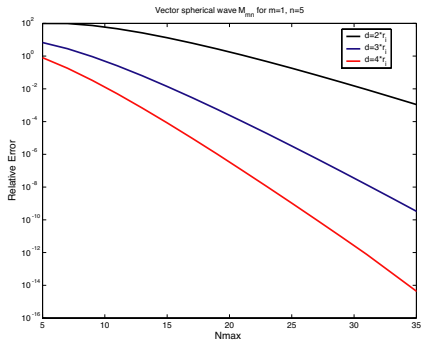

Figure 5. Relative errors due to truncations in applying addition theorem for various r_{ji} where r_i is 1.

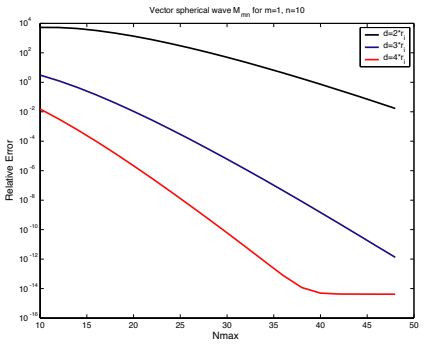

Figure 6. Relative errors due to truncations in applying addition theorem for various r_{ji} where r_i is 3.

Bearing the impact of truncation errors in applying the translational addition theorems and T-matrix approach, when the eccentricity of the scatterer is large, the iterative procedure may

become an ill-conditioned one, for which caution needs to be taken. We use a method similar to the successive over-relaxation method (SOR), which takes the form of a weighted average between the previous iterate and the computed new iterate successively for each component as reported in [53] where multi-sphere system was considered. An extrapolation factor w ($0 \leq w \leq 1$) is used to speed up the convergency procedure.

6. NUMERICAL RESULTS

In this section, we compare the theoretical predictions of the proposed iterative approach with numerical simulations, as well as measurements for scattering from dielectric circular cylinders with finite length. For cases where the ratio of horizontal to rotational axes ρ, the equal-volume sphere radius r_v and the refractive index fall in the region where the conventional EBCM is applicable, we expect that our proposed method should provide comparable results. To test this preposition, various size parameters of cylinders are used with r_v ranging from 0.5 to 3, ρ from 1 to 1/3, and the refractive index is $1.5 + 0.02i$. For linear polarization the scattering cross section is defined as

$$\sigma_{pq} = 4\pi \left| F_{pq}(\hat{k}_s, \hat{k}_i) \right|^2, \tag{42}$$

and for circular polarization

$$\sigma = \pi \left| F_{vv}\left(\hat{k}_s, \hat{k}_i\right) \pm F_{hh}\left(\hat{k}_s, \hat{k}_i\right) \right|^2 \tag{43}$$

where the $+$ and $-$ signs stand for left-hand and right-hand circular polarization, respectively.

The results are shown in Figs. 7–12. One can observe from the figures that both the vertically-polarized and horizontally-polarized bistatic scattering cross sections obtained by our method are in perfect agreements with that of T-matrix approach when r_v is smaller than 3.

Table 2. Parameters for the samples.

Sample	①	②	③	④
ka	0.1143	0.1904	0.2666	0.3428
c/a	10.00	9.99	9.99	10.00
$\mathrm{Re}(\epsilon)$	3.13	3.13	3.15	3.14

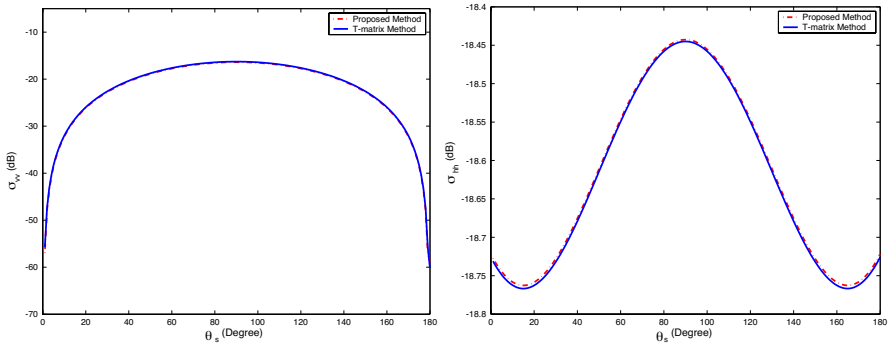

(a) Vertical polarization (b) Horizontal polarization

Figure 7. The bistatic scattering cross section of a cylinder under our proposed method and EBCM at broadside incidence where r_v is 0.5 and ρ is 1/2.

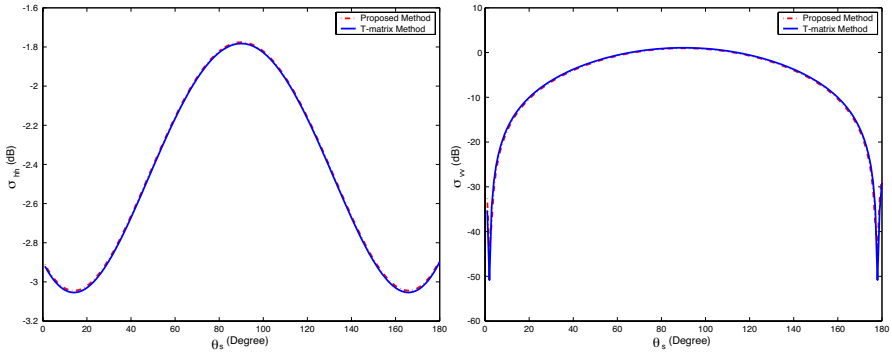

(a) Vertical polarization (b) Horizontal polarization

Figure 8. The bistatic scattering cross section of a cylinder under our proposed method and EBCM at broadside incidence where r_v is 1 and ρ is 1/2.

Comparison between the theoretical predictions of our method and experimental data is shown in Fig. 13, where the experimental data are taken from [42] for different samples with the parameters listed in Table 2. The imaginary part of dielectric constant is $0.036i$. The overall agreement is good except at locations near the null where the experimental results are much higher. Similar discrepancy with the GRG approximation was also reported by Karam et al. [22] where they suggested that the discrepancy may be due to the finite equivalent

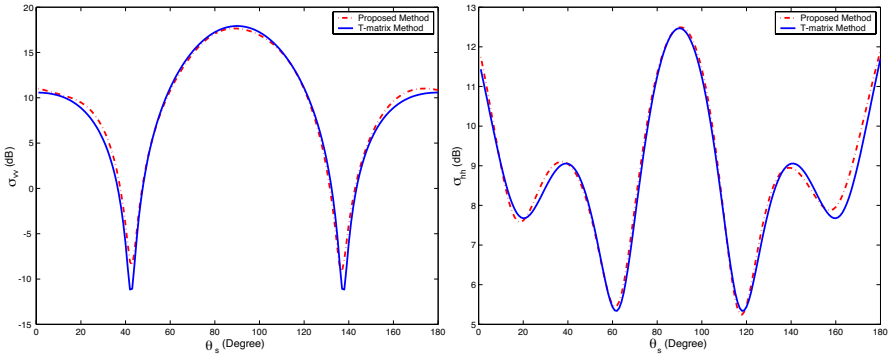

(a) Vertical polarization (b) Horizontal polarization

Figure 9. The bistatic scattering cross section of a cylinder under our proposed method and EBCM at broadside incidence where r_v is 3 and ρ is 1/2.

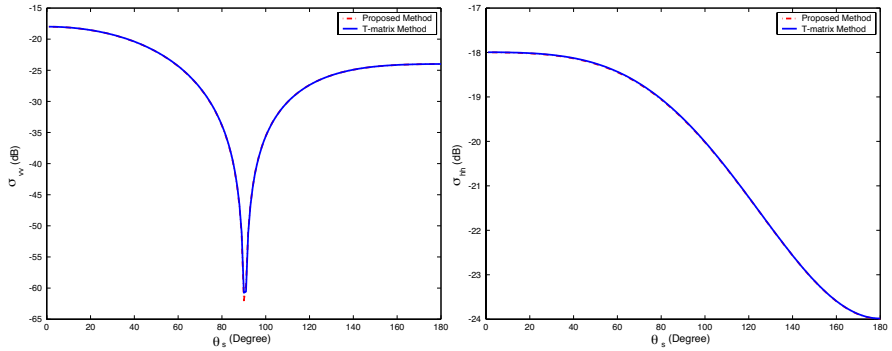

(a) Vertical polarization (b) Horizontal polarization

Figure 10. The bistatic scattering cross section of a cylinder under our proposed method and EBCM at end-fire incidence where r_v is 0.5 and ρ is 1/3.

bandwidth of the measurement system. In addition, they expected this difference not to be important when dealing with scattering from randomly oriented cylinders where returns from volumes are summed incoherently. It is clear from Fig. 13 that our method outperforms the GRG approximation.

Finally we compare the backscattering coefficients obtained from our proposed method for both vertical and horizontal polarizations

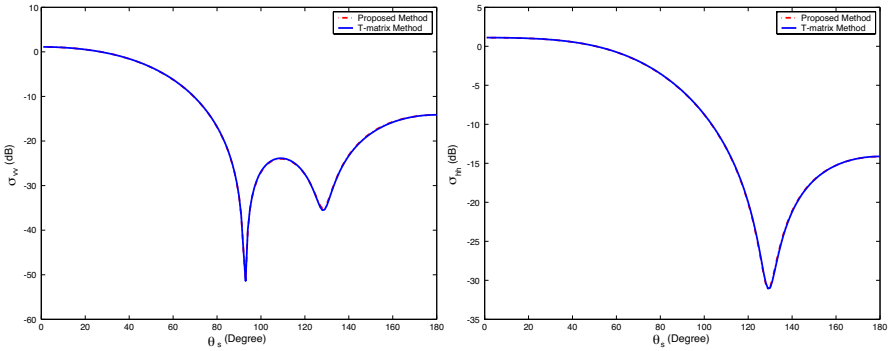

(a) Vertical polarization (b) Horizontal polarization

Figure 11. The bistatic scattering cross section of a cylinder under our proposed method and EBCM at end-fire incidence where r_v is 1 and ρ is 1/3.

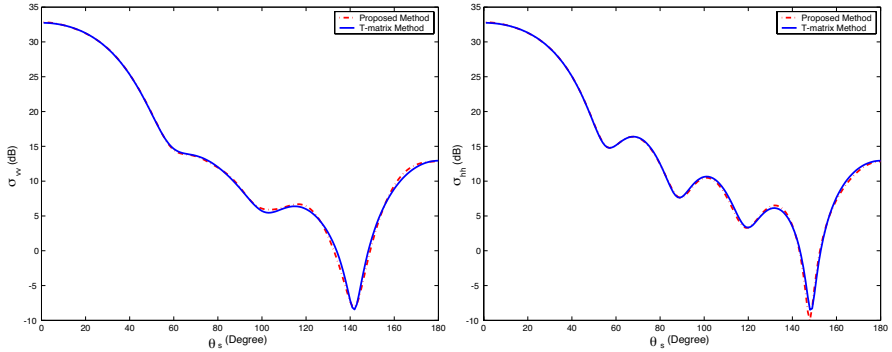

(a) Vertical polarization (b) Horizontal polarization

Figure 12. The bistatic scattering cross section of a cylinder under our proposed method and EBCM at end-fire incidence where r_v is 3 and ρ is 1/3.

with that by GRG approximation when it is applicable. Fig. 14 illustrates the results for a needle case, where ka is 0.7, ρ is 1/25 and the refractive index is $1.5 + 0.02i$. The results show good agreement between the two methods.

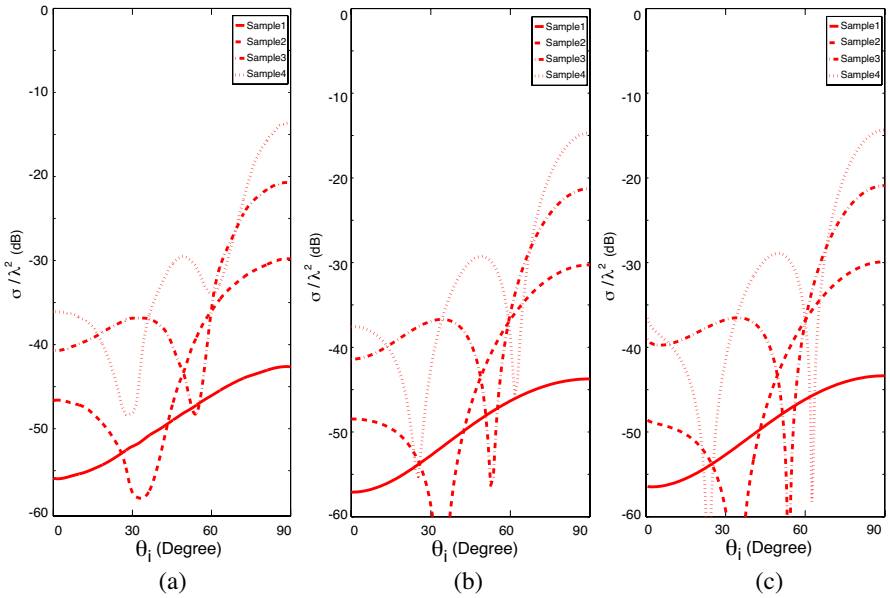

Figure 13. Comparisons among our proposed method, GRG approximation and the measured backscattering cross section of dielectric cylinders excited by a circularly polarized plane wave. (a) Measurement datas. (b) Prediction by our method. (c) Predictions by Karam.

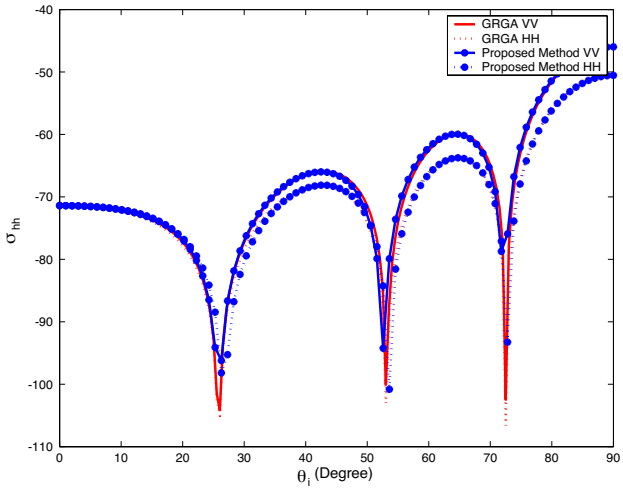

Figure 14. Comparison of backscattering cross sections of a cylinder between our proposed method and GRG approximation.

Table 3. This list includes the variables in this paper.

Variable	Definition
$Rg\bar{M}_{mn}, Rg\bar{N}_{mn}$	regular vector spherical waves
$\bar{M}_{mn}, \bar{N}_{mn}$	outgoing vector spherical waves
$\bar{a}^{inc}$	incident field coefficients
$\bar{a}^{sca}$	scattered field coefficients
ψ_{mn}	scalar wave function
P_n^m	associated Legendre function
z_n	spherical Bessel function or spherical Hankel function
$a(m,n,\mu,\nu,p)$	Gaunt coefficient
C^{mn}	scalar translational coefficient
$A_{\mu\nu}^{mn}, B_{\mu\nu}^{mn}$	vector translational coefficient
S_{ip}	primary surface of sub-cylinder i
S_{ij}	interface between sub-cylinder i and j
$\bar{a}_{mn}^{(i)p}$	primary coefficients of sub-cylinder i
$a_{mn}^{s(i)p}$	primary scattered field coefficients of sub-cylinder i
$\bar{a}_{mn}^{(i)u}$	upper tangential field coefficients on the interface of sub-cylinder i
$\bar{a}_{mn}^{s(i)u}$	upper tangential scattered field coefficients on the interface of sub-cylinder i
$\bar{a}_{mn}^{(i)d}$	lower tangential field coefficients on the interface of sub-cylinder i
$\bar{a}_{mn}^{s(i)d}$	lower tangential scattered field coefficients on the interface of sub-cylinder i
$F_{pq}(\hat{k}_s, \hat{k}_i)$	amplitude scattering matrix
$\hat{p}$	unit polarizations for the incident wave
$\hat{q}$	unit polarizations for the scattered wave
ρ	ratio of horizontal to rotational axes
r_v	equal-volume sphere radius
σ	scattering cross section

7. CONCLUSION

In this paper, we proposed a new iterative technique to analyze scattering from dielectric circular cylinders with finite length. It was demonstrated that the new method can extend regular T-matrix approach to solve cylindrical cases with large aspect ratio. The new method can also be used for finite dielectric cylinders with arbitrary cross section as long as the T matrix of each sub-cylinder can be accurately obtained. Moreover, the new method holds the potential for multi-cylinder problems, especially for the cases of closely positioned cylinders.

ACKNOWLEDGMENT

This work was partly supported by China National Science Foundation under Grant No. 40571114 and Zhejiang Science Foundation under Grant No. Y106443.

REFERENCES

1. Ulaby, F. T., K. Sarabandi, K. McDonald, M. Whitt, and M. C. Dobson, "Michigan microwave canopy scattering model," *Int. J. Remote Sensing*, Vol. 38, No. 7, 2097–2128, 2000.
2. Yueh, S. H., J. A. Kong, J. K. Jao, R. T. Shin, and T. L. Toan, "Branching model for vegetation," *IEEE Trans. Geosci. Remote Sensing*, Vol. 30, 390–402, 1992.
3. Chen, Z., L. Tsang, and G. Zhang, "Appication of stochastic lindenmayer systems to the study of collective and cluster scattering in microwave remote sensing of vegetation," *Progress In Electromagnetics Research*, PIER 14, 233–277, 1996.
4. Chiu, T. and K. Sarabandi, "Electromagnetic scattering from short branching vegetation," *IEEE Trans. Geosci. Remote Sensing,* Vol. 38, No. 2, 911–925, 2000.
5. Du, Y., Y. L. Luo, W. Z. Yan, and J. A. Kong, "An electromagnetic scattering model for soybean canopy," *Progress In Electromagnetics Research*, Vol. 79, 209–223, 2008.
6. Jin, J. M., V. V. Liepa, and C. T. Tai, "A volume-surface integral equation for electromagnetic scattering by inhomogeneous cylinders," *J. Electromagn. Waves and Appl.*, Vol. 2, 573–588, 1988.
7. Elsherbeni, A. Z., M. Hamid, and G. Tian, "Iterative scattering of a Gaussian beam by an array of circular conducting and dielectric cylinders," *J. Electromagn. Waves and Appl.*, Vol. 7, 1323–1342, 1993.
8. Konistis, K. and J. L. Tsalamengas, "Plane wave scattering by an array of bianisotropic cylinders enclosed by another one in an unbounded bianisotropic space: Oblique incidence," *J. Electromagn. Waves and Appl.*, Vol. 11, 1073–1090, 1997.
9. Naqvi, Q. A. and A. A. Rizvi, "Low contrast circular cylinder buried in a grounded dielectric layer," *J. Electromagn. Waves and Appl.*, Vol. 12, 1527–1536, 1998.
10. Wang, L. F., J. A. Kong, K. H. Ding, T. Le Toan, F. Ribbes, and N. Floury, "Electromagnetic scattering model for rice canopy based on Monte Carlo simulation," *Progress In Electromagnetics Research*, PIER 52, 153–171, 2005.
11. Arslan, A. N., J. Pulliainen, and M. Hallikainen, "Observations of L- and C-band backscatter and a semi-empirical backscattering model approach from a forest-snow-ground system," *Progress In Electromagnetics Research*, PIER 56, 263–281, 2006.
12. Ruppin, R., "Scattering of electromagnetic radiation by a perfect

electromagnetic conductor cylinder," *J. Electromagn. Waves and Appl.*, Vol. 20, 1853–1860, 2006.

13. Hamid, A. K., "Multi-dielectric loaded axially slotted antenna on circular or elliptic cylinder," *J. Electromagn. Waves and Appl.*, Vol. 20, 1259–1271, 2007.
14. Henin, B. H., A. Z. Elsherbeni, and M. H. Al Sharkawy, "Oblique incidence plane wave scattering from an array of circular dielectric cylinders," *Progress In Electromagnetics Research*, PIER 68, 261–279, 2007.
15. Zhang, Y. J. and E. P. Li, "Fast multipole accelerated scattering matrix method for multiple scattering of a large number of cylinders," *Progress In Electromagnetics Research*, PIER 72, 105–126, 2007.
16. Valagiannopoulos, C. A., "Electromagnetic scattering from two eccentric metamaterial cylinders with frequency-dependent permittivities differing slightly each other," *Progress In Electromagnetics Research B*, Vol. 3, 23–34, 2008.
17. Illahi, A., M. Afzaal, and Q. A. Naqvi, "Scattering of dipole field by a perfect electromagnetic conductor cylinder," *Progress In Electromagnetics Research Letters*, Vol. 4, 43–53, 2008.
18. Svezhentsev, A. Y., "Some far field features of cylindrical microstrip antenna on an electrically small cylinder," *Progress In Electromagnetics Research B*, Vol. 7, 223–244, 2008.
19. Ahmed, S. and Q. A. Naqvi, "Electromagnetic scattering from a perfect electromagnetic conductor cylinder buried in a dielectric half-space," *Progress In Electromagnetics Research*, PIER 78, 25–38, 2008.
20. Yeh, C., R. Woo, A. Ishimaru, and J. Armstrong, "Scattering by single ice needles and plates at 30 GHz," *Radio Sci.*, Vol. 17, 1503–1510, 1982.
21. Schiffer, R. and K. O. Thielheim, "Light scattering by dielectric needles and disks," *J. Appl. Phys.*, Vol. 50, No. 4, 2476–2483, 1979.
22. Karam, M. A. and A. K. Fung, "Electromagnetic wave scattering from some vegetation samples," *IEEE Trans. Geosci. Remote Sensing,* Vol. 26, 799–808, 1988.
23. Karam, M. A. and A. K. Fung, "Electromagnetic wave scattering from some vegetation samples," *Int. J. Remote Sensing*, Vol. 9, 1109–1134, 1988.
24. Stiles, J. M. and K. Sarabandi, "A scattering model for thin dielectric cylinders of arbitrary crosssection and electrical length,"

IEEE Trans. Antennas Propag., Vol. 44, 260–266, 1996.

25. Waterman, P. C., "Matrix formulation of electromagnetic scattering," *Proc. IEEE*, Vol. 53, 805–811, 1956.
26. Mishchenko, M. I. and L. D. Travis, "T-matrix computations of light scattering by large spheroidal particles," *Opt. Commun.*, Vol. 109, 16–21, 1994.
27. Roussel, H., W. C. Chew, F. Jouvie, and W. Tabbara, "Electromagnetic scattering from dielectric and magnetic gratings of fibers: A T-matrix solution," *J. Electromagn. Waves and Appl.*, Vol. 10, 109–127, 1996.
28. Mishchenko, M. I., L. D. Travis, and A. Macke, "Scattering of light by polydisperse, randomly oriented, finite circular cylinders," *Appl. Opt.*, Vol. 35, 4927–4940, 1996.
29. Mishchenko, M. I., L. D. Travis, and D. W. Mackowski, "T-matrix computations of light scattering by nonspherical particles: A review," *J. Quant. Spectrosc. Radiat. Transfer*, Vol. 55, 535–575, 1996.
30. Wielaard, D. J., M. I. Mishchenko, A. Macke, and B. E. Carlson, "Improved T-matrix computations for large, nonabsorbing and weakly absorbing nonspherical particles and comparison with geometrical optics approximation," *Appl. Opt.*, Vol. 36, 4305–4313, 1997.
31. Mishchenko, M. I., "Calculation of the amplitude matrix for a nonspherical particle in a fixed orientation," *Appl. Opt.,* Vol. 39, 1026–1031, 2000.
32. Barber, P. W., "Resonance electromagnetic absorption by nonspherical dielectric objects," *IEEE Trans. Microwave Theory Tech.*, Vol. 25, 373–371, 1954.
33. Iskander, M., A. Lakhtakia, and C. Durney, "A new procedure for improving the solution stability and extending the frequency range of the EBCM," *IEEE Trans. Antennas Propag.*, Vol. 31, 317–324, 1983.
34. Kahnert, F. M., "Numerical methods in electromagnetic scattering theory," *J. Quant. Spectrosc. Radiat. Transfer*, Vol. 79–80, No. 2, 755–824, 2003.
35. Al-Rizzo, H. M. and J. M. Tranquilla, "Electromagnetic wave scattering by highly elongated and geometrically composite objects of large size parameters: The generalized multipole technique," *Appl. Opt.*, Vol. 34, 3502–3521, 1995.
36. Doicu, A. and T. Wriedt, "Calculation of the T matrix in the null-field method with discrete sources," *J. Opt. Soc. Am.*, Vol. 16,

2539–2544, 1999.

37. Eremina, E., Y. Eremin, and T. Wriedt, "Extension of the discrete sources method to light scattering by highly elongated finite cylinders," *J. Modern Opt.*, Vol. 51, No. 3, 423–435, 2004.
38. Pulbere, S. and T. Wriedt, "Light scattering by cylindrical fibers with high aspect ratio using the null-field method with discrete sources," *Part. Part. Syst. Charact.*, Vol. 21, 213–218, 2004.
39. Wriedt, T., R. Schuh, and A. Doicu, "Scattering by aggregated fibres using a multiple scattering T-matrix approach," *Part. Part. Syst. Charact.*, Vol. 25, 74–83, 2008.
40. Tsang, L., J. A. Kong, and R. T. Shin, *Theory of Microwave Remote Sensing*, Wiley Interscience, New York, 1985.
41. Tsang, L., J. A. Kong, K. H. Ding, and C. O. Ao, *Scattering of Electromagnetic Waves — Numerical Simulations*, John Wiley & Sons, Inc., New York, 2001.
42. Allan, L. E. and G. M. McCormick, "Measurements of the backscatter matrix of dielectric bodies," *IEEE Trans. Antennas Propag.*, Vol. 28, No. 2, 166–169, 1980.
43. Friedman, B. and J. Russek, "Addition theorems for spherical waves," *Q. Appl. Math.*, Vol. 12, 13–23, 1954.
44. Stein, S., "Addition theorems for spherical ware functions," *Q. Appl. Math.*, Vol. 19, 15–24, 1961.
45. Gaunt, J. A., "On the triplets of helium," *Philos. Trans. R. Soc. Lond. A*, Vol. 228, 151–196, 1929.
46. Brunning, J. H. and Y. T. Lo, "Multiple scattering of EM waves by spheres. Part I and II," *IEEE Trans. Antennas Propag.*, Vol. 19, No. 3, 378–400, 1971.
47. Mackowski, D. W., "Analysis of radiative scattering for multiple sphere configurations," *Proc. R. Soc. Lond. A*, 599–614, 1991.
48. Chew, W. C., "Recurrence relations for three-dimensional scalar addition theorem," *J. Electromagnetic Waves Appl.*, Vol. 6, 133–142, 1992.
49. Cruzan, O. R., "Translational addition theorems for spherical vector ware functions," *Q. Appl. Math.*, Vol. 20, 33–39, 1962.
50. Tsang, L. and J. A. Kong, "Effective propagation constant for coherent electromagnetic waves in media embedded with dielectric scatterers," *J. Appl. Phys.*, Vol. 11, 7162–7173, 1982.
51. Koc, S., J. M. Song, and W. C. Chew, "Error analysis for the numerical evaluation of the diagonal forms of the scalar spherical addition theorem," *SIAM J. Numer. Anal.*, Vol. 36, No. 3, 906–921, 1999.

52. Mishchenko, M. I., "Light scattering by size-shape distributions of randomly oriented axially symmetric particles of size comparable to a wavelength," *Appl. Opt.*, Vol. 32, 4652–4666, 1993.
53. Xu, Y. L., "Electromagnetic scattering by an aggregate of spheres," *Appl. Opt.*, Vol. 34, 4573–4588, 1995.